

MODIS Infrared Sea Surface Temperature Algorithm
Algorithm Theoretical Basis Document
Version 1.0

Submitted by

Otis B. Brown
Peter J. Minnett
University of Miami
Miami, FL 33149-1098

Under Contract Number NAS5-31361

21 October 1996

Table of Contents

| | |
|---|-----------|
| Preface..... | v |
| 1.0 Introduction..... | 1 |
| 1.1 Algorithm and Product Identification..... | 1 |
| 1.2 Algorithm Overview..... | 1 |
| 1.3 Document Scope | 2 |
| 1.4 Applicable Documents and Publications..... | 2 |
| 2.0 Overview and Background Information..... | 2 |
| 2.1 Experimental Objective..... | 3 |
| 2.2 Historical Perspective | 3 |
| 2.3 Instrument Characteristics | 4 |
| 3.0 Algorithm Description | 5 |
| 3.1 Theoretical Description..... | 5 |
| 3.1.1 Physics of the Problem | 7 |
| 3.1.2 Mathematical Aspects of the Algorithm | 12 |
| 3.1.3 Variance or Uncertainty Estimates | 12 |
| 3.2 Practical Considerations..... | 13 |
| 3.2.1 Algorithm Builds | 14 |
| 3.2.2 Reprocessing | 14 |
| 3.2.3 Programming/Procedural Considerations | 15 |
| 4.0 Calibration and Algorithm Validation..... | 15 |
| 4.1 Post-launch Algorithm Through Validation | 15 |
| 4.1.1 Scientific Objectives..... | 16 |
| 4.1.2 Missions | 17 |
| 4.1.3 Science data products | 18 |
| 4.2 Validation Criteria..... | 18 |
| 4.2.1 Validation Approach | 18 |
| 4.2.2 Sampling requirements and trade-offs..... | 19 |
| 4.2.3 Measures of success..... | 22 |
| 4.3 Pre-launch algorithm and test/development activities..... | 22 |

| | |
|---|-----------|
| 4.3.1 Field experiments and studies..... | 22 |
| 4.3.2 Operational surface networks | 25 |
| 4.3.3 Existing satellite data | 26 |
| 4.4 Post-launch activities | 26 |
| 4.4.1 Planned field activities and studies..... | 26 |
| 4.4.2 New-EOS Targeted coordinated field campaigns..... | 27 |
| 4.4.3 Needs for other satellite data..... | 28 |
| 4.4.4 Measurement needs (<i>in situ</i>) at calibration / validation sites..... | 29 |
| 4.4.5 Needs for instrument development..... | 29 |
| 4.4.6 Geometric registration site..... | 29 |
| 4.4.7 Intercomparisons (Multi-instrument) | 29 |
| 4.5 Implementation of validation results in data production | 30 |
| 4.5.1 Approach..... | 30 |
| 4.5.2 Role of EOSDIS | 30 |
| 4.5.3 Plans for archival of validation data..... | 30 |
| 5.0 Validation using <i>in situ</i> sea surface temperature measurements | 31 |
| 5.1 Sources of <i>in situ</i> SSTs and other environmental variables..... | 31 |
| 5.2 MODIS Data Extractions | 32 |
| 5.2.1 Time Coordinates | 33 |
| 5.3 Matchup Procedures..... | 33 |
| 5.3.1 Filtering Records..... | 33 |
| 5.3.2 First-guess satellite-derived SST | 36 |
| 5.4 Matchup database definition..... | 36 |
| 5.5 Quality Control and Diagnostics..... | 37 |
| 5.5.1 Running Climatology Approach..... | 37 |
| 5.5.2 Space/time Coherence | 38 |
| 5.6 Implications for the ECS, TLCF and MOTCF Efforts..... | 38 |
| 5.7 Exception Handling | 39 |
| 5.8 Data Dependencies..... | 39 |
| 5.9 Output Product..... | 40 |
| 6.0 Constraints, Limitations, Assumptions..... | 41 |
| 7.0 References..... | 41 |

Tables

| | |
|---|----|
| Table 1. Bands for MODIS Infrared SST Determination..... | 4 |
| Table 2. Channel characteristics of satellite-borne infrared radiometers..... | 28 |
| Table 3. Sources of <i>in situ</i> SST Values to be Included in the MODIS..... Sea_sfc Temperature Algorithm Matchup Databases | 31 |
| Table 4. Fields included in global matchup database (version 1). | 34 |
| Table 5. Fields included in North American matchup database (version 1). | 35 |
| Table 6 MODIS IR SST Climatology Dataset..... | 38 |
| Table 7. MODIS Sea_sfc Data Dependencies..... | 39 |
| Table 8. MODIS IR SST Quality Assessment Product..... | 40 |
| Table 9. MODIS IR SST Output Product 2527 | 40 |

Preface

This Algorithm Theoretical Basis Document (ATBD) describes our current working model of the algorithm for estimating bulk sea surface temperatures from the MODIS mid- and far-infrared bands. While effort has been made to make this document as complete as possible, it should be recognized that algorithm development is an evolving process. This document is a description of the prototype algorithm for MODIS sea surface temperature estimation as it currently exists.

As will be seen from the document, there are areas which still require substantial research effort before finalization. In particular we are assuming that complementary development efforts by Dr. Robert Evans' MODIS activity will provide much of the implementation information needed for data flow and operational computer codes.

The NOAA/AVHRR results described in this document are based on continuing joint development and tests associated with the NASA/NOAA Pathfinder AVHRR Oceans activity. Experience gained with the Pathfinder efforts is directly assisting development of the MODIS comparison database with respect to design, testing and implementation.

1.0 Introduction

The Earth Observing System (*EOS*) Moderate Resolution Imaging Spectrometer (*MODIS*) is a satellite based visible/infrared radiometer for the sensing of terrestrial and oceanic phenomena. The *MODIS* design builds on the heritage of several decades of NOAA infrared radiometer use [Schwalb, 1973; 1978]. An aspect of our efforts as members of the *MODIS* instrument team is to develop a state-of-the-art algorithm for the estimation of sea surface temperature (*SST*). The goal of this document is to describe the prototype pre-launch *SST* algorithm for the *MODIS* instrument, version1. Included in this description are physical aspects of the approach, calibration and validation needs, quality assurance, *SST* product definition and unresolved issues.

1.1 Algorithm and Product Identification

SST estimates produced by the proto-algorithm will be labeled version 1. This is a level 2 product with *EOSdis* product number 2527; it is *MODIS* product number 28, labeled *Sea_sfc* Temperature.

1.2 Algorithm Overview

This algorithm is being developed on the *MODIS* Ocean Team Computing Facility (*MOTCF*) for use in the *EOS* Data and Information System (*EOSdis*) core processing system. The *Sea_sfc* Temperature determination is based on satellite infrared retrievals of ocean temperature which are corrected for atmospheric absorption using combinations of several *MODIS* mid- and far-infrared channels. Cloud screening is based on two approaches: use of the cloud screening product (3660) and a cloud indicator derived during the *SST* retrieval. The latter approach consists of individual retrievals passing a series of negative threshold, spatial homogeneity, and delta-climatology tests. The quality assessment *SST* output products are vectors composed of the estimated *SST* value, input calibrated radiances and derived brightness temperatures for each channel, flags which quantify the cloud screening results, scan coordinate information, latitude, longitude and time. The distributed *Sea_sfc* Temperature product consists of vectors composed of the *SST* estimate, latitude, longitude, time and quality assessment flags.

1.3 Document Scope

This document describes the physical basis for the Sea_sfc Temperature algorithm, gives the structure of the current version 1 algorithm, discusses implementation dependencies on other observing streams, and describes validation needs.

This replaces version 0.4, dated 10 November 1994, and differs from the earlier document by including a more detailed account of the validation plans.

1.4 Applicable Documents and Publications

MODIS SST Proposal, 1990, Infrared Algorithm Development for Ocean Observations with EOS/MODIS, Otis B. Brown

MODIS IR SST Execution Phase Proposal, 1991, Infrared Algorithm Development for Ocean Observations with EOS/MODIS, Otis B. Brown

2.0 Overview and Background Information

The importance of satellite-based measurements to study the global distribution and variability of sea surface temperature has been described in the MODIS Instrument Panel Report [MODIS, 1986] and elsewhere [ESSC, 1988; WOCE, 1985; Weller and Taylor, 1993], and will not be discussed here. Suffice it to say that global surface temperature fields are required on daily to weekly time scales at moderate resolution, *i.e.*, 10-200 km. Since the pioneering work of Anding and Kauth [1970] and Prabhakara *et al.*, [1974] it has been known that atmospheric water vapor absorption effects in the infrared can be corrected with high accuracy using linear combinations of multiple channel measurements. MODIS specifications ensure very low radiometer noise ($<0.05\text{K}$ between $10\text{ }\mu\text{m}$ - $12\text{ }\mu\text{m}$), as well as narrow, well placed windows in the $3.7\text{ }\mu\text{m}$ - $4.2\text{ }\mu\text{m}$ band. These enhancements, together with new radiative transfer modeling tuned to the MODIS channel selection, should permit global SST retrievals on space scales of $\sim 10\text{ km}$ with RMS errors $\leq 0.45\text{K}$ for weekly fields at mid-latitudes with errors $\leq 0.5\text{K}$ in the tropics. Such fields are a necessary prerequisite to achieve the stated goal of accuracies at the 0.2°C level for $2^\circ \times 2^\circ$ squares [Weller and Taylor, 1993].

2.1 Experimental Objective

This algorithm development activity is part of a larger MODIS Instrument Team investigation to develop accurate methods for determination of ocean sea surface temperature, generate mapped SST fields, validate their characteristics, determine the principal modes of spatial and temporal variation for these fields, and develop a sequence of simple models to assimilate such fields to study specific scientific problems such as global warming. The proposed efforts will directly address the upper ocean mixed layer and permit computation of seasonally varying thermal fields to be used in both the Joint Global Ocean Flux Study (JGOFS)[GOFS, 1984] and World Ocean Circulation Experiment (WOCE)[WOCE, 1985] programs. These fields can be used to provide indices for ocean warming on seasonal to interannual scales and, thus, will directly address NASA Earth System Science objectives [ESSC, 1988]. Due to the complexity of the calibration, atmospheric correction, and data assimilation aspects of these fields, the overall effort requires close collaboration with other proposed EOS efforts with respect to the MODIS and ADEOS NSCAT measurement systems.

2.2 Historical Perspective

Development of algorithms for the production of reliable SST data sets from space borne infrared radiometers has been pursued by a number of investigators, agencies and governments since the late 1960's [see review by Brown and Cheney, 1983, and Abbott and Chelton, 1991, for details]. For example, NOAA [McClain, 1981; McClain *et al.*, 1983; Strong and McClain, 1984; McClain *et al.*, 1985], NASA [Shenk and Salomonson, 1972; Chahine, 1980; Susskind *et al.*, 1984], and RAL/UK [Llewellyn-Jones, *et al.*, 1984] address infrared radiometry, using a variety of radiation transfer codes, model and observed vertical distributions of temperature and moisture, and actual observations. Minnett [1986; 1990 and Barton (1995)] summarize the present state of the art for high quality retrievals from NOAA/AVHRR (Advanced Very High Resolution Radiometer) class instruments. The current state of the art is limited by radiometer window placement, radiometer noise, quality of pre-launch instrument characterization, inflight calibration quality, viewing geometry, and the atmospheric correction.

2.3 Instrument Characteristics

MODIS has a number of infrared channels in the mid- and far-infrared which were placed to optimize their use for SST determination. Bands of particular utility to infrared SST determination are listed in Table 1.

Table 1. Bands for MODIS Infrared SST Determination

| Band Number | Band Center (μ) | Bandwidth (μ) | NE Δ T (K) |
|-------------|-----------------------|---------------------|-------------------|
| 20 | 3.750 | 0.1800 | 0.05 |
| 22 | 3.959 | 0.0594 | 0.07 |
| 23 | 4.050 | 0.0608 | 0.07 |
| 31 | 11.030 | 0.5000 | 0.05 |
| 32 | 12.020 | 0.5000 | 0.05 |

These bands were chosen for MODIS based on particular aspects of the atmospheric total column transmissivity in each part of the mid- and far-infrared spectrum. Figure 1 presents a profile of the expected earth radiance at satellite height from 3 μ m to 14 μ m.

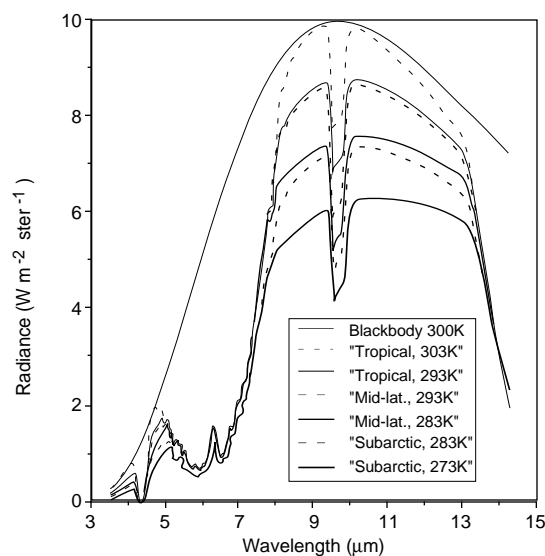


Figure 1. Earth radiance in the mid- to far-infrared spectrum. The various curves give a range of expected infrared radiances for a variety of typical atmospheres and surface temperatures. A 300K blackbody curve is provided to permit visual comparison of the path length absorption for the various cases. Profile data is computed by the Lowtran radiative transfer program [Selby *et al.*, 1978].

The bands located near 4 μ m (20, 22, and 23) exhibit high sensitivity (defined as $\frac{1}{L} \frac{dL}{dT}$) and are placed where the influence of column water vapor is minimal on the sensed radiances. Bands in the far-infrared between 10 μ and 12 μ (31 and 32) are located near the maximum emission for a 300K blackbody (an approximation for the average Earth temperature) and placed such that there is a significant difference in the band integrated water vapor absorption for the two bands. The mid-infrared bands, while having minimal water vapor loading, suffer from decreased available Earth radiance, narrow bandwidth and possible specularly reflected solar radiance during daylight. The far-infrared bands are near the maximum of the Earth's emission and have larger bandwidth, but are burdened by large water vapor absorption in the tropical air masses. The mid- and far-infrared bands differing sensitivity to total column water vapor complement each other and provide a balanced infrared SST observing strategy. The specified NE Δ T for each band is ≤ 0.07 K. As will be seen, these characteristics are necessary prerequisites for accurate SST determination at the desired level of accuracy.

3.0 Algorithm Description

This section describes the proto-MODIS infrared algorithm. It includes a theoretical overview, a physical basis for the approach, and several sub-sections which discuss implementation and accuracy issues.

3.1 Theoretical Description

Given well-calibrated radiances from MODIS, deriving accurate sea surface temperature fields and associated statistics is dependent on one's abilities to correct for the effects of the intervening atmosphere on these spectral radiances and to provide assimilation mechanisms which cover the time-space windows of interest. Sensing SST through the atmosphere in the thermal infrared is subject to several environmental factors which degrade the accuracy of the perceived temperature. Major sources of error in the radiometric determination are (a) sun glint (MODIS channels 20, 22, and 23), (b) water vapor absorption in the atmosphere (MODIS channels 31, 32), (c) trace gas absorption (all channels) and (d) episodic variations in aerosol absorption due to volcanic eruptions, terrigenous dust blown out to sea, etc. (all channels). Although satellite radiometers sense the ocean's radiation temperature known as "skin" temperature, satellite results are commonly compared with bulk temperature measurements in the upper several meters of the ocean. Air-sea interaction modifies

the relationship between these two variables and causes observable differences in the bulk and radiation temperatures [Robinson, *et al.*, 1984; Cornillon and Stramma, 1985; Schluessel, *et al.*, 1990]. We must be prepared to quantify regional and temporal differences between bulk and skin temperatures. This is one of the goals of the *in situ* SST calibration and validation activity.

The integrated atmospheric transmissivity over each of the MODIS infrared channels [20, 22, 23, 31, 32] differs. Consequently, algorithms can be constructed which depend on the differences in measured temperature among these channels [Anding and Kauth, 1970]. The simplest such algorithm assumes that, for small cumulative amounts of water vapor, the atmosphere is sufficiently optically thin that the difference between the measured temperature in any channel and the true surface temperature can be parameterized as a simple function of the difference between the measured temperatures in two channels with different atmospheric transmissions.

We are using the line-by-line numerical radiative transfer code developed at Rutherford Appleton Laboratory in the UK as a basis for modeling atmospheric absorption processes in the MODIS infrared bands: [Llewellyn-Jones, *et al.*, 1984; Zavody, *et al.*, 1995]

Linear algorithms (MCSST) are based on a formula of the following form for the surface temperature T_s :

$$T_s = \alpha + \beta T_i + \gamma(T_i - T_j) \quad (1)$$

where the T_i 's are brightness temperatures in various channels for a given location and the coefficients α , β and γ give the parameterized correction [Deschamps and Phulpin, 1980; Llewellyn-Jones *et al.*, 1984], or can be derived empirically from good composite sets of surface and satellite observations [Prabhakara, *et al.*, 1974]. In Eq. (1) such an algorithm constructed on channels 31 and 32 would replace i, j by 31, 32 respectively. Equivalent relations can be constructed for any two channel pairs. α , β and γ values are -1, 1, and 3, respectively, for a typical AVHRR 4,5 algorithm (T_s in °C) [McClain *et al.*, 1983].

Although Eq. (1) is easy to implement, it does not permit correction for changes in air mass due to scan-angle. Llewellyn-Jones *et al.*, [1984] develop a table from numerical simulations which permits modification of Eq. (1) into a form:

$$T_s = \alpha + \beta' T_i + \gamma'(T_i - T_j) + \delta (1 - \sec(\theta)) \quad (2)$$

where θ is the zenith angle and δ is an additional scan angle coefficient. This approach reduces the errors at large scan angles for moist atmospheres by more than 1K.

For MODIS Sea_sfc Temperature estimation (proto-algorithm) we will eventually implement a correction equation which is a variation of Eq. (2) for multiple pairs of the available bands (see Section 3.1.1). This will be coupled with an objective criterion based on observed retrieval scatter for a local region determine which channel combination(s) is(are) used. We will also examine the possibility of implementing a version of NLSST technique [Walton *et al.*, 1990] which provides a nonlinear approach to atmospheric correction.

3.1.1 Physics of the Problem

It has been noted that satellite infrared radiances can be straightforwardly corrected for atmospheric absorption in the water vapor bands by utilizing a split (or dual) window technique. In this and the following discussions we will assume that bands are chosen such that water vapor is the primary variable absorbing gas, O₃ variation is minimal, the column is cloud free, and specularly reflected sunlight is not present. We outline a theoretical basis for the split or dual window methods. Split and dual window refer to use of two channels in the 10 μ m-12 μ m band (split) or to two channels in the 4 μ m and 10 μ m-12 μ m bands (dual) and follows Deschamps and Phulpin [1980]. This derivation is for a nadir view through an atmosphere, which can be characterized by species invariant, vertically integrated absorbents. In practice it has been shown that this simplification of the problem will address scan angles within 30° of the nadir and all but the most moist tropical atmospheres (see Fig. 2a).

It is easily shown that, for a non-scattering atmosphere, the outgoing infrared radiance at the top of the atmosphere in the mid- and far-infrared, normal to the earth, can be represented by:

$$L_{\lambda} = L_{\lambda} (Surface) t_{\lambda} (O, P_o) - \int_o^{P_o} B_{\lambda} [T(P)] dt_{\lambda} (O, P), \quad (3)$$

where L_{λ} is the radiance, $t_{\lambda} (0, P_x)$ the transmissivity from a pressure level P_x to the top of the atmosphere, and $B_{\lambda} (T)$ the Planck function. This neglects the small contribution of energy emitted by the atmosphere downwards, and reflected into the upwelling beam at the sea surface. Following Deschamps and Phulpin [1980] this can be written as:

$$\Delta L_{\lambda} = B_{\lambda} (T_o) - L_{\lambda} \quad (4)$$

$$= \int_o^{P_o} [B_{\lambda} (T_o) - B_{\lambda} (T(P))] dt_{\lambda} (O, P) \quad (5)$$

i.e., ΔL_{λ} is the radiance error introduced by the atmosphere. Equivalently we can write this as a temperature deficit:

$$\Delta T_{\lambda} = T_o - T_{\lambda} \quad (6)$$

Relating the temperature T_{λ} to the radiance $L_{\lambda} (T)$ by the Planck function we find:

$$\Delta T_{\lambda} = \frac{\Delta L_{\lambda}}{(\partial B / \partial T)|_{T_o}} \quad (7)$$

For an optically thin gas the following approximations can be made:

$$dt_{\lambda} (O, P) \cong -k_{\lambda} dU(P) \quad (8)$$

where k_{λ} is the absorption coefficient at wavelength, λ , and $U(P)$ is the optical path-length of the gas from the top of the atmosphere to pressure level P .

Secondly, we assume that the Planck function is adequately represented by a first order Taylor series expansion in each channel window, *i.e.*,

$$B_{\lambda} [T(P)] = B_{\lambda} (T_o) + \left(\frac{\partial B_{\lambda}}{\partial T} \right) \bigg|_{T_o} [T(P) - T_o] \quad (9)$$

Upon substitution of (7), (8) and (9) into (5) we see

$$\Delta T = k_{\lambda} \int_0^{P_0} [T_0 - T(P)] dU(P), \quad (10)$$

that is, the error is partitioned into a strict function of k_{λ} and a wavelength independent integral over atmospheric parameters. Thus, if one picks two spectral regions of the atmosphere, one has two linear equations with different k_{λ} 's to solve simultaneously.

For a two channel system we can represent the SST as

$$T_s = a_0 + a_1 T_1 + a_2 T_2 \quad (11)$$

with a_0 being included as an overall adjustment for wavelength independent attenuation. a_1 and a_2 are theoretically, as above, or empirically determined constants dependent on the optical absorption in the two radiometer channels. This is a simple transformation of Eq. (1) with $a_0 = \alpha$, $a_1 = \beta + \gamma$, and $a_2 = -\gamma$.

Such linear algorithms have been used for the split and dual windows between 10 μm and 12 μm bands [McClain *et al.*, 1983, 1985, and others]. Various workers have shown that it is difficult to have the best performance in a specific locale with a globally tuned algorithm, *i.e.*, an algorithm that has been tuned over a large number of atmospheric states does not show optimum performance in a regional study [*e.g.*, Minnett, 1990]. It is apparent from the derivation that this is due to the assumptions about the vertical distribution of water vapor and the invariance of k_{λ} . In practice, one finds that the largest outliers are for extreme temperature, humidity, or scan angle situations.

Figure 2a shows departures from linearity between *in situ* surface bulk temperatures and space derived sea surface temperatures based on a linear algorithm such as Eq. 11. It is readily seen that the major departures from linearity are at high temperatures.

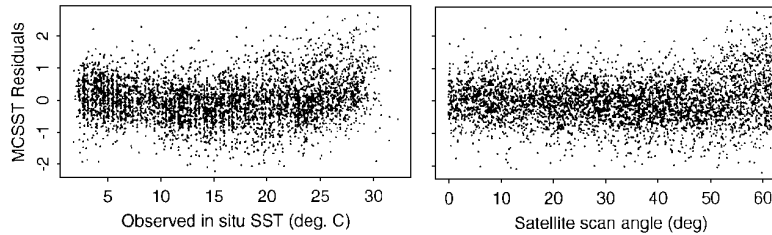


Figure 2. Comparison of MCSST SST estimates with fixed buoy observations taken from the AVHRR analog of the “North American” matchup database. MCSST coefficients $a_0 = -0.0024$, $a_1 = 3.53$, $a_2 = -2.52$. RMS difference of the ensemble is 0.66C. Figure 2a. Residual *vs.* *in situ* temperature. Figure 2b. Residual *vs.* satellite scan angle

For temperature residuals shown in Fig. 2a, the envelope shows greater span and positive residual bias for temperatures greater than 25°C. While the dependence on scan angle in Fig. 2b is minimal for angles less than 50°, there is a dramatic expansion of the envelope and a positive trend apparent for larger angles. The two aspects of the MCSST algorithms displayed in Fig. 2 are the principal reason for examining other algorithms with improved high temperature, large air mass characteristics. The angular dependence of the residuals results from the inherent non-linearity of the radiative transfer process, the emission-angle dependence of the surface emissivity, neglected in the linear algorithm derivation, and the reflection of downwelling sky radiation.

While there have been a number of different methods employed to address this problem, the simplest approach currently available is to characterize the large air mass, *i.e.*, absorption cases, by adding a constant multiplying an angular function to the SST estimator. The correction equation in Eq. 2 is an example of this approach. In general, for a two-channel system, one uses an estimator of the form:

$$T_S = a_0 + a_1 T_1 + a_2 T_2 + a_3 f(\theta) \quad (12)$$

where $f(\theta)$ is some appropriately chosen function of scan or zenith angle. This form, however, while improving the error behavior at large scan angles, does not adequately control the residual behavior at high temperatures.

A further generalization of this approach is to posit a non-linear structure for the SST estimator. As a starting point for this investigation, we define a NLSST (non-linear SST) atmospheric equation following Walton [1990]. The NLSST algorithm is a derivative of the CPSST (cross-product SST) algorithm [Walton, 1988] and forms the basis of the current AVHRR SST retrievals. Our working definition uses the form:

$$T_S = a_0' + a_1' T_1 + a_2' (T_1 - T_2) \cdot T_b + a_3' (\sec \theta - 1) \quad (13)$$

where the terms T_S , and T_i are as defined in Eq. 12, and T_b is the environmental temperature. While Eq. 13 can be viewed as a generalization of Eq. 12, there is a notable departure from the MCSST form. The inclusion of an environmental temperature, T_b , as a multiplier for a brightness temperature difference between the two channels provides a different behavior at higher temperatures.

Figs. 3a and 3b present the results of a matchup comparison with fixed buoy data off the US East Coast using Eq. 12 as the SST estimator. The improvement in behavior at both high temperatures and large air masses is apparent. For the matchup data set considered this approach provides an improvement of about 20%, or 0.13C in the error residual. A problem with implementing this version of the algorithm is the T_b term. One must have a estimate of the temperature for the pixel within $\pm 2\sigma$ prior to estimating its value. Typically this is done using a climatology or an MCSST type algorithm as a first guess.

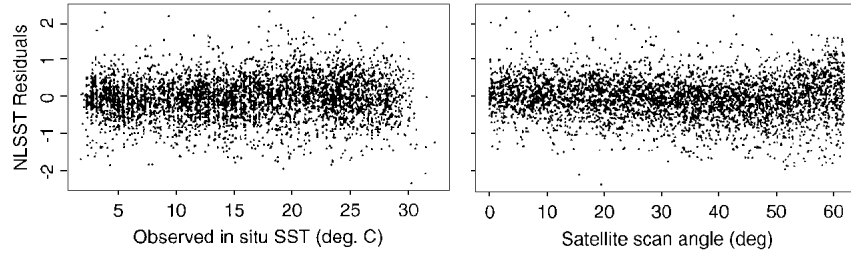


Figure 3. NLSST atmospheric correction algorithm comparison with *in situ* buoy data based on the AVHRR analog of the “North American” matchup database. NLSST coefficients are $a_0' = 1.42$, $a_1' = 0.94$, $a_2' = 0.098$ and $a_3' = 0.88$. The RMS of the difference ensemble is 0.53C. Fig. 3a. Residuals *vs.* *in situ* temperature. Fig. 3b. Residuals *vs.* satellite scan angle.

Eq. 13 will be the form of the delivered proto-algorithm. That is, we will furnish the coefficients and $f(\theta)$ computed to retrieve an optimal Sea_sfc Temperature for combinations of bands, two at a time. We expect this algorithm to improve based on sufficient iteration between model and *in situ* validation results. Current testing with NOAA-9 AVHRR SST estimates suggests that Eq. 13 for two channels placed in the 10 μm to 12 μm window can provide estimates of SST with RMS errors at the 0.5K-0.6K level.

Experience with the AVHRR Ocean Pathfinder data has shown that to achieve these levels of accuracy it is necessary to use time-dependent coefficients in the NLSST algorithm. These are slowly varying, being weighted means over a three-month interval. The benefit of using regionally varying coefficients has not yet been demonstrated.

Current details of the AVHRR Ocean Pathfinder Matchup Database [Podestá *et al.*, 1996] can be found on the WWW at URL <http://www.rsmas.miami.edu/~gui/matchups.html>.

Development work planned (and proposed) over the next several years will enhance this SST estimation equation in several ways. First, by using the new MODIS bands around 4 μm we will implement a set of split window algorithms which should work markedly better in very moist, tropical atmospheres. Second, we will explore the use of higher order nonlinear algorithms. Third, as the calibration-validation database coverage is enlarged, we will develop a parallel set of SST skin temperature algorithms based on this formalism.

3.1.2 Mathematical Aspects of the Algorithm

Implementation of this algorithm is straightforward. There are no particular mathematical issues which must be resolved for successful implementation of the current algorithm.

3.1.3 Variance or Uncertainty Estimates

The uncertainty in the MODIS IR SST retrieval is straightforward to calculate. Taking Eq. 11 and performing an error analysis, one sees that the error in T_s can be represented as:

$$e_t = \sqrt{\sum_{i=1}^n a_i e_i^2} \quad (14)$$

where e_t is the total error, a_i are the estimation coefficients, and e_i is the error apparent for each channel i used in the algorithm. e_i is given by

$$e_i = \sqrt{(e_i^a)^2 + (NE\Delta T_i)^2} \quad (15)$$

with e_i^a being the error due to atmospheric correction and $NE\Delta T_i$ deriving from instrumental design and performance considerations. Since the constants a_i are order 1, and one assumes that the nadir and/or atmospheric errors are comparable and the various bands have similar characteristics, one can see the error scales as

$$e_t = \sqrt{n} e_i \quad (16)$$

where n is the number of bands used.

This analysis makes clear the fact that calibration and/or atmosphere correction errors are important components of the error budget, *i.e.*, 0.1K of error in calibration for a band is effectively an rms error in a dual channel algorithm of 0.14K, assuming perfect atmospheric correction. Therefore, we have requested that the calibration be demonstrably accurate at the choice of 0.05K level to minimize the effect of calibration errors. The best atmospheric correction currently available for ATSR suggests that errors due to atmospheric correction in optimal cases for a nadir viewing instrument are approximately 0.3K [Mutlow, *et al.*, 1994; Minnett, 1990; Barton, *et al.*, 1993; Minnett, 1995b].

If one assumes that the calibration errors and the atmospheric errors are random and thus can be RSS'd, as in the preceding analysis, one sees that expected errors of 0.35K-0.4K in the result are the best that can be expected for two-channel configurations. This equation also points out that there is a cost associated with adding more bands to improve atmospheric correction. In addition to providing information potentially useful for correcting the effects of the intervening atmosphere, each additional channel also introduces noise into the SST retrieval.

3.2 Practical Considerations

Major areas of concern have to do with efficient implementation of the atmospheric correction codes. Given that a minimum of 7×10^8 pixels with 9 radiances must be processed daily (Order 10^{10} estimates), the calculation must be highly optimized - this implies an average processing of 10^4 pixels \cdot sec⁻¹ just to stay current. Current proto-algorithm development benchmarking suggests that much of the calculation must be table driven and close attention must be addressed to efficient, fast mass storage access for the algorithm to be effectively implemented.

Specific aspects of the implementation include calculation of the black body temperature and efficient mechanisms for estimating temperature from radiances. The black body formula to be used is

$$B_T(\nu) = 1.19106759 \times 10^{-5} \nu^3 \left[e^{1.43879 \nu/T} - 1 \right]^{-1} \quad (17)$$

where v is the wavenumber in cm^{-1} , T is the temperature in K, and B is resultant blackbody radiance. Since this product requires level-1a calibrated radiances as inputs to the calculation, there is no specific calibration procedure. Now, we assume that the output of each MODIS infrared channel count is proportional to input radiance, *i.e.*,

$$C_i = S_i L_i + I_i \quad (18)$$

with C_i the count, L_i the incident radiance, and S_i , I_i the slope and intercepts for the i th channel [Lauritson *et al.*, 1979 and Brown *et al.*, 1985] provide analogous descriptions for NOAA AVHRR radiance computation].

Effective arithmetic implementation of the calibration step necessitates development of a counts-to-temperature look-up table which is computed one time and then offset, depending on changes in instrument internal operating temperature. Functionally one performs the following calculation:

$$T_B = \text{table}(i) \quad (19)$$

where T_B is the respective brightness temperature for the channel in question and table is the counts to brightness temperature look-up table.

3.2.1 Algorithm Builds

This document describes the proto-prelaunch algorithm. There will be additional versions of the Sea_sfc Algorithm. The overall structure of the algorithm should remain reasonably stable, *i.e.*, we expect the correction equation to be based on a combination of MODIS infrared bands. Our execution phase plan identifies a number of releases prior and post-launch.

3.2.2 Reprocessing

Provided there is no ‘catastrophic’ change to the atmosphere, such as a large volcanic eruption that injects large amounts of aerosols into the stratosphere, MODIS atmospheric correction algorithms will not change very quickly, however, our execution phase plan suggests that annual updates should be expected. All MODIS Sea_sfc Temperature Algorithm products should be identified with a version identification so

that users can readily discern the algorithm used. We would propose that major reprocessing of MODIS infrared data be no more frequent than annual. Catastrophic atmospheric events will be dealt with, if they occur, in the best fashion possible.

3.2.3 Programming/Procedural Considerations

Programming/procedural considerations will be addressed in MOTCF trial algorithm implementation effort led by MODIS Instrument Team member Dr. Robert Evans. We have no better information than was last stated on processing estimates. Trial implementation in the MOTCF will be the basis of improved processing estimates.

4.0 Calibration and Algorithm Validation

Calibration/Validation has two important aspects: prelaunch determination of instrument calibration and characterization in a thermal-vacuum test setting and validation of on-orbit performance. We assume that our role in the pre-launch efforts is an advisory role, *i.e.*, the MCST calibration and characterization activity will directly supervise the thermal-vacuum activities and deliver models to transform MODIS sensor counts into calibrated radiances which are valid over the on-orbit operating envelope.

On-orbit performance characterization consists of two aspects: assessing calibration model performance and assessing MODIS Sea_sfc Temperature algorithm performance. We assume that radiance calculated from instrument counts will be accomplished using calibration models provided by the MCST Calibration activity. We assume that conversion to radiances is a reversible transformation from counts, *i.e.*, no information is lost in going to and from counts to radiances. Please note, however, that raw count data will be required for selected sites in the calibration-validation effort. We will require access to the MCST calibration performance results in order to characterize the impact of the on-orbit calibration model performance on the algorithm performance.

4.1 Post-launch Algorithm Through Validation

The infrared channels of MODIS form a self-calibrating radiometer. By using measurements of cold space and of an on-board black-body calibration target, the infrared measurements from the earth-scan are calibrated producing radiances in the spectral intervals defined by the system response functions of each channel. These

calibrated radiances can be converted to brightness temperatures (*i.e.*, the temperature of a black-body that would give the same channel radiance) at the height of the satellite. To derive an oceanic surface temperature from the calibrated radiances at satellite height (or top-of-atmosphere brightness temperatures) it is necessary to correct for the effects of the intervening atmosphere. This is the role of the sea-surface temperature retrieval algorithm, sometimes referred to as the atmospheric correction algorithm.

The post-launch validation activities are designed primarily to test the efficacy of the sea-surface temperature retrieval algorithm, not primarily to validate the pre-launch characterization or in the in-flight calibration procedure. It is presumed that the pre-launch tests, supplemented by in-flight maneuvers, will provide adequate characterization of the instrument to engender confidence in the calibrated channel radiance measurements. With this confidence, the validation measurements can be interpreted in terms of the performance of the atmospheric correction algorithm; without this confidence the separation between instrument performance and algorithm performance cannot be made and the interpretation of the validation data sets will be very difficult. Of particular importance in the pre-launch characterization are the determination of the spectral response functions of the MODIS channels, the quantification of “cross-talk” between channels, and the accurate description of the properties of the scan mirror as they change with scan angle. Failure to correctly characterize these before launch will seriously compromise our ability to understand the properties, strengths as well as weaknesses, of the SST retrieval algorithm and to demonstrate the validity of the derived SST fields.

4.1.1 Scientific Objectives

Several fundamentally different, but complementary, data sets are needed to provide an adequate sampling of the marine atmospheric conditions and sea-surface temperature (SST) that is necessary to validate the MODIS infrared channel measurements and derived SST fields. Our validation strategy is two-fold: Highly-focused field expeditions using state-of-the-art calibrated spectral radiometers, supported by extensive instrument suites to determine the state of the atmosphere, are necessary to understand the atmospheric and oceanic processes that limit the accuracy of the derived SST. In addition, long-time period, global-scale data sets are necessary to provide a monitoring capability that would reveal calibration drift and the consequences of

sudden or extreme atmospheric events, such as volcanic eruptions, transoceanic transport of terrestrial aerosols, cold-air outbreaks, *etc.* on the global SST product.

4.1.2 Missions

MODIS, and derivative instruments, are expected to be operational for about 15 years beginning with the launch of the AM-1 platform in 1998. It is our intent to use field programs that take place during the pre-launch and operational period as the basis of MODIS validation exercises. In particular, the DOE ARM (Atmospheric Radiation Measurements) program sites in the Tropical Western Pacific Ocean (TWP) and North Slope of Alaska and Adjacent Arctic Ocean (NSA-AAO) provide a valuable framework for MODIS validation as they provide an unparalleled selection of instruments to determine the state of the atmosphere [Stokes and Schwartz, 1994]¹. These sites will operate for about a decade, beginning in late 1996 for the TWP, and about one year later for the NSA-AAO, at the extreme ranges of atmospheric and oceanic conditions. In addition to these two long-term sites, use will be made of the supplementary, oceanic ARM sites that are intended to be operated on a short-term basis, intermittently or for specific research campaigns. These include the eastern North Pacific or Atlantic Oceans (probably the Azores), the Gulf Stream off the eastern USA, and the Bering or Greenland Seas.

Opportunities to use other oceanic and marine atmospheric campaigns based on ships, buoys, fixed platforms, aircraft, and island stations will be grasped as funding and resources allow.

Pre-launch campaigns are being used to test strategies, constraints, and to develop the instrumental and computational tools that will be used in the post-launch validation, again as opportunities and funding allow. Examples of these include the Combined Sensor Program cruise to the Tropical Western Pacific in March-April 1996, the Aerosol Characterization Experiments (ACE) in the Pacific and Atlantic Oceans, and the International North Water Polynya expeditions planned for 1997 and 1998.

¹ The first ARM Site, currently operational and situated in the Southern Great Plains centered near Lamont, OK, and other supplementary terrestrial sites, provide a valuable source of measurements for validation of land surface temperature: this parameter is not dealt with here.

4.1.3 Science data products

The primary science data product to be validated is sea-surface temperature (MODIS Product number 28 / EOSDIS Product number 2527). To achieve this requires thorough characterization of the atmospheric and ocean surface variables that influence the SST retrieval from the MODIS channel radiance measurements. The cloud mask to be provided by the MODIS Atmospheres Group (Paul Menzel) (EOSDIS Product number 3660) will be used to eliminate cloud contamination, but the influence of clear-air constituents, including aerosols, remains to be corrected. At the sea surface, the spectral emissivity together with its surface roughness and emission angle dependences must be taken into account. The sea-surface temperature retrieval is of course limited to the ice-free oceans: the ice-mask product (MODIS MOD29) will be used to delineate the ice-free areas.

4.2 Validation Criteria

Post-launch validation of the MODIS infrared channels is required to monitor the performance of the in-flight calibration procedure to detect possible degradation, to uncover potential instrument problems (such as possibly inadequate characterization of the angular dependent reflectivity of the scan mirror), but primarily to determine the effectiveness of the atmospheric correction algorithm. Ideally the accuracy and noise characteristics of the data being used in the validations should be superior to those of the MODIS measurements. This may be difficult to achieve, given the expected performance of MODIS.

4.2.1 Validation Approach

Validation is required over the lifetimes of the MODIS missions, and, the validating instruments must be deployed in situations that encompass the entire range of surface temperatures and atmospheric variability. Since no single approach provides a perfect validation measurement, a selection of techniques and instruments is required to provide an adequate validation data set. The approach includes (i) validation of top-of-the-atmosphere radiances, (ii) validation of surface radiances and (iii) validation of surface temperatures.

There are three possible methods of validating the top-of-atmosphere radiances:

- comparison with other satellite measurements
- comparison with aircraft radiometers underflying the satellite,

- using radiative transfer modeling to simulate the MODIS measurements.

Validation of surface radiances is achieved using calibrated spectroradiometers, such as the Marine-Atmospheric Emitted Radiance Interferometer [Smith *et al.*, 1996], or broad-band infrared thermometers. These instruments can be mounted on low-flying aircraft [Saunders and Minnett, 1990; Rudman *et al.*, 1994; Smith *et al.*, 1994], ships [Schluessel *et al.*, 1987; Smith *et al.*, 1996], or fixed platforms.

using *in situ* measurements employ those taken using conventional thermometers on free-drifting or moored buoys [Strong and McClain, 1984; Podestá *et al.*, 1997], and ships [e.g. Llewellyn-Jones *et al.*, 1984].

Wherever possible, synergism will be sought by collaboration with the validation efforts of the MODIS Ocean Color and MODIS Atmospheres groups, to leverage equipment and data.

4.2.2 Sampling requirements and trade-offs

Comparison with other satellite infrared radiometers has the advantage of comparing similar measurements. The problems in such an approach are in the possible changes in the top-of-the atmosphere radiation field between the two satellite overpasses (resulting from changes in the surface temperature and/or in the intervening atmosphere), differences in the viewing geometry of the two satellites, differences in the spectral responses of the different satellite instrument channels, and possibly inadequate accuracy or noise characteristics of the validating instrument. Another possible problem is the potential for undetected in-flight degradation of the validating radiometer - if systematic discrepancies are found it may not be apparent which satellite sensor is at fault.

A significant advantage of using aircraft radiometers is that the data can be taken simultaneously with the MODIS measurements. However, because of the difference in spacecraft and aircraft speeds, truly coincident measurements will be very few, but within, say a 30-minute window of the satellite overpass a large number of validation measurements could be obtained, (precise interval to be determined; Minnett, [1990]). Also, the aircraft radiometers can be arranged (in principle) to match the MODIS viewing geometry, and can be scheduled (again, in principle) to avoid conditions that would make data interpretation difficult (e.g., broken cloud fields). Disadvantages of

this technique include the effects of the atmosphere above the aircraft, which can be accounted for by modeling using an assumed (or measured) temperature and humidity profile, and the accuracy of the aircraft instruments. Candidate aircraft instruments for top-of-the atmosphere radiance validation of the channels used in SST determination include the MAS (MODIS Airborne Simulator; King and Herring, [1992]) and the HIS (High-Resolution Interferometer Sounder; [Bradshaw and Fuelberg, 1993]. These instruments are flown typically on the NASA ER-2 research aircraft at a height of ~20km, and under these conditions the spatial resolution is 50m (MAS) and 2km (HIS). The noise levels of the instruments are not as low as those for the MODIS infrared channels (see table in 4.3). For the MAS the NE Δ T is ~0.3K for a target at ~290K for the 3.7-4.0 μ m channels and 0.1 - 0.2K for the 11-12 μ m channels, but these could be greatly improved (by a factor of 20 if the noise were truly random) by averaging the data down to the MODIS spatial resolution of ~1km². The noise levels in the HIS spectra in the 800 to 1050 cm⁻¹ interval are typically 0.2-0.45 mW m⁻² sr⁻¹ cm, and these result in an uncertainty in the skin SST retrieved from the HIS spectra of ~0.15K [Nalli, 1995].

The use of numerical models of the radiative transfer through the atmosphere to simulate the satellite measurements requires high quality measurements of the relevant atmospheric properties (temperature and humidity profiles, aerosol characteristics) and emitted radiance at the surface taken at the time of the satellite overpass. Advantages of this approach are that a large data-base of measurements can be generated over an extended period of time and representing a large range of atmospheric conditions, surface temperatures, and viewing geometries for relatively modest outlay. Disadvantages are the uncertain accuracies of the atmospheric profiles, generally derived from routine radiosonde measurements [Schmidlin, 1988], and shortcomings in the parameterization of incompletely understood physical processes in the radiative transfer model, such as the atmospheric water vapor anomalous continuum absorption and emission, and the effects of tropospheric and stratospheric aerosols.

The long-term measurement of surface emitted radiance, or the channel brightness temperatures, at the surface serves to monitor the behavior of the atmospheric correction algorithms as well as the MODIS performance. The surface measurement is of emitted radiance plus the reflected component of the downwelling radiance originating in the atmosphere. The MODIS space based measurement is of this combination, after attenuation by atmospheric absorption and scattering, plus the radiance emitted or scattered by the atmosphere into the MODIS field of view. This

validation measurement is therefore less direct than a top-of-atmosphere comparison. Surface measurements can be related to the MODIS measurement by using a radiative transfer model to provide an estimate of the atmospheric attenuation and upwelling and scattered radiation, or by converting the surface measurement to a temperature and comparing it with the surface temperature derived from the MODIS measurements. In either case, the successful interpretation requires a good description of the atmospheric and surface properties (skin SST, surface emissivity and wind speed). In the latter case a measure of the downwelling radiation is required to derive the temperature from the surface measurements. This can be achieved by pointing the surface radiometer at the sky. Suitable instruments include the AERI (Atmospheric Emitted Radiation Interferometer) or, for use at sea, the Marine-AERI (M-AERI), and broad-band infrared thermometers [Smith *et al.*, 1996]. The M-AERIs have internal black-body calibration targets and so provide a calibrated measurement. They measure the spectrum of infrared radiation in the range from 3.3 to 18 μm with a spectral resolution of $\sim 0.5 \text{ cm}^{-1}$. These spectra can be compared to the MODIS measurements by multiplying them by the MODIS normalized channel spectral response functions. The M-AERI spectra can also be analyzed to derive surface temperature and emissivity, and, using spectra of sky radiation, the temperature and humidity structure of the atmosphere.

Broad-band infrared radiation thermometers have the advantage over (M)AERI's in that they are inexpensive. They usually do not have the required accuracy of 0(0.1K) and have a simple internal calibration procedure (if any). However, recent experience with some types indicates they may produce useful observations, and may be suitable for deployment in larger numbers on platforms of opportunity.

Surface temperature thermometers can be deployed in plentiful numbers to provide adequate monitoring of MODIS performance in principle. However, they have a big disadvantage in that their measurement may be decoupled from the MODIS measurement by near-surface temperature gradients. For sea surface temperature the in situ thermometer is immersed in the water, frequently at depths of 0(1m) and its measurement may differ from the temperature of the radiating skin of the ocean by $>1\text{K}$. These gradients are caused by heat exchange between ocean and atmosphere [the skin effect; *e.g.* Robinson *et al.*, 1984; Schluessel *et al.*, 1990] or by diurnal heating in conditions of low wind speed and therefore reduced surface mixing [*e.g.* Stramma *et al.*, 1986]. Despite this problem in situ thermometers have been used extensively to

validate satellite SST's [e.g. Strong and McClain, 1984; Llewellyn-Jones *et al.*, 1984; Podestá *et al.*, 1997].

4.2.3 Measures of success

The results of the validations will be used to revise the atmospheric correction algorithms used in the SST derivation. The algorithms will be refined until the accuracy goals of the MODIS mission have been reached, in as much as this can be demonstrated within the constraints imposed by the methods of determining the absolute accuracy of the MODIS SST measurement.

4.3 Pre-launch algorithm and test/development activities

An extremely important aspect of the pre-launch activities is the full characterization of the infrared channels of the MODIS flight models. This includes giving a complete definition of the spectral and spatial responses of the individual channels; specifying the properties of the elements used in the in-flight calibration procedure, and providing a good description of the thermal conditions expected in and around the instrument in orbit. Without this information, the interpretation of the data derived from the validation exercises will be very difficult.

Pre-launch validation activities will be directed towards fine-tuning the atmospheric correction algorithm, refining validation instruments and determining the best strategies for the post-flight validation.

4.3.1 Field experiments and studies

The primary instrument for the surface validation of the MODIS infrared channels is the M-AERI, and part of the pre-launch activities will be directed to ensuring the accuracy of the instrument, testing it under sea-going conditions, and developing the necessary software.

A prototype instrument has already been used at sea for a proof-of-concept experiment in the Gulf of Mexico in January 1995, where it performed very well. It demonstrated an ability to measure skin temperatures that agreed well with near-surface *in situ* measurements, and deviated in the manner expected from consideration of surface heat exchanges. The M-AERI data could also be analyzed to derive the angular-dependent spectral emissivity of the ocean surface, and its measurements of the sky radiation

could be inverted to produce profiles of temperature and humidity in the lower atmosphere [Smith *et al.*, 1996]. Building on the experiences of this cruise, a more rugged M-AERI has been developed at the Space Science and Engineering Center of the University of Wisconsin at Madison. This instrument was used during the Combined Sensor Program (CSP) cruise in the Tropical Western Pacific in spring 1996. In addition to testing the instrument in extreme conditions, this cruise furnished an extremely valuable data set to study the effects of the tropical atmosphere on infrared satellite SST measurements including the spatial and temporal correlation characteristics of the relevant atmospheric constituent, the near-surface horizontal and vertical thermal gradients. Fig. 4 shows independent measurements of sea surface temperature taken at a station in the Tropical Western Pacific from the NOAA's *Discoverer*. The thin line that makes excursions for high temperatures is an *in situ* measurement taken from a float at a depth of ~0.1m; the dark line that does not reach high temperatures is an *in situ* measurement at 5m depth. The two other lines are skin temperature measurements taken by the M-AERI at the infrared wavelengths shown at 55° zenith angle. The wind was very light during the day (local time is UTC+9.5h) and a strong diurnal thermocline built up during the day. At night this was eroded by corrective mixing and the two *in situ* temperatures converge. During both night and day the skin temperature is cooler by up to a few tenths of a degree. While the diurnal thermocline in this example is rather extreme, the skin gradients are typical, illustrating the need to include them in the validation of MODIS SST products. The skin gradients are a significant fraction of the MODIS SST error budget. The first M-AERI will be delivered to the University of Miami in January 1997.

A subsequent opportunity to use the M-AERI in an extreme environment is presented by the proposed International North Water Polynya project, in which it is planned that research ice-breakers will have extended cruises in the area at the north of Baffin Bay in 1997 and 1998. Other cruise opportunities will be sought that would enable the pre-launch deployment of the M-AERI in a range of atmospheric and oceanic conditions.

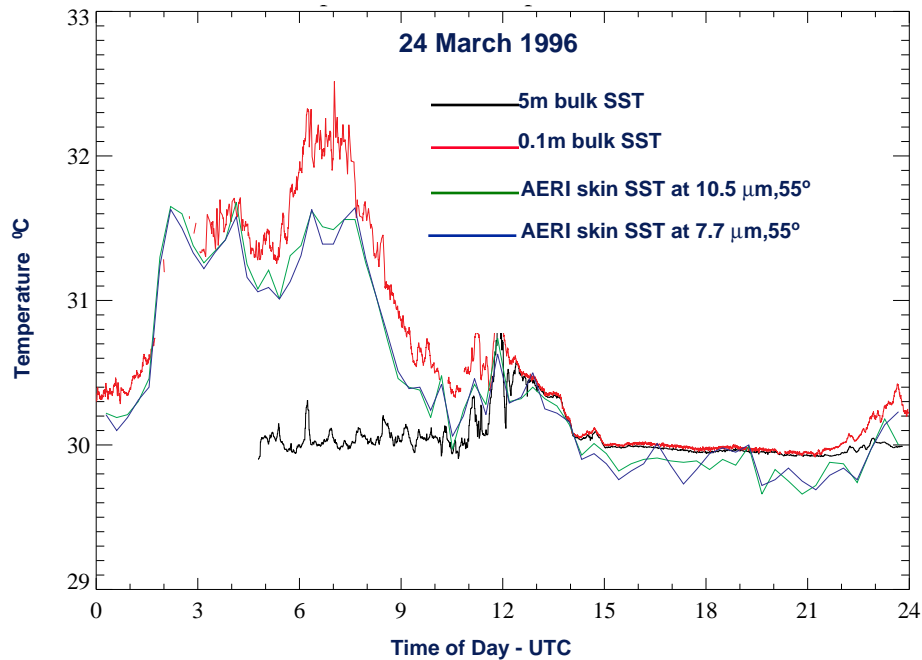


Figure 4. CSP Cruise, NOAA S Discoverer – Tropical Western Pacific

Additional opportunities to use the M-AERI may be available during the cruises to service the MOBY (Marine Optical Buoy) situated off Hawaii, which is a keystone in the MODIS Ocean Color validation plan. These cruises (D. Clark, MODIS P.I) provide the opportunity to sample sub-tropical atmospheric conditions around the seasons.

An alternative method of M-AERI deployment would be on a research platform, preferably one that experiences a range of meteorological conditions. Candidate platforms are in the Gulf of Mexico, southern North Sea, Florida Current, Mediterranean Sea, and off Australia. A fixed platform would enable long-term M-AERI deployment and relatively easier logistics than a ship deployment, but would probably require outfitting the platform with instruments to provide the ancillary atmospheric and surface oceanic measurements. The possibility of using such platforms for both pre- and post-launch validation activities will be explored.

Since only two M-AERIs are foreseen to be available for MODIS validation, they are by necessity going to be limited in their deployments. A complementary approach is to use many, simpler and commercially available, broad-band infrared thermometers on ships of opportunity and fixed platforms. Part of the pre-launch validation activities will be

directed towards an evaluation of the performance of such instruments and devising a strategy for implementing such a program, should resources permit .

For pre-launch aircraft campaigns, it is envisaged that collaboration with the MODIS Atmospheres Group will provide some opportunities for flights over the oceans. Such campaigns would permit the assessment of the applicability of aircraft instruments, such as the MAS and HIS (see 4.2.2 above).

The atmospheric correction algorithm that will be applied to the MODIS measurements to derive SST will be derived pre-launch by radiative transfer modeling to simulate the MODIS infrared channel measurements [e.g. Llewellyn-Jones *et al.*, 1984; Barton *et al.*, 1989]. The success of atmospheric correction algorithms derived from simulated satellite measurements based on radiative transfer modeling hinges on (amongst other things - see 4.2.2 above) how well the set of atmospheric profiles used in the simulations represents the distribution of conditions over which the algorithm will be subsequently applied. Biases in the distribution of atmospheric conditions represented by the radiosondes will translate into biases in the retrieved SST fields [Minnett, 1996]. Effort must be invested in attempting to building a high-quality representative marine radiosonde set.

Another activity in the pre-launch period will be to study the near-surface vertical temperature gradients that, under certain circumstances, can decouple the skin temperature from an in situ measurement at a meter or so below the surface. These effects will be studied in field campaigns using the M-AERI and in situ thermometers [e.g., Smith *et al.*, 1996] and using existing “climatology” and parameterizations to determine the spatial and temporal distributions of significant gradients that might adversely influence MODIS SST validation.

4.3.2 Operational surface networks

Selected radiosoundings from the operational network of meteorological observing stations will be used to define the global distributions of the atmospheric temperature and water vapor profiles for use in MODIS infrared channel simulations for the development of the atmospheric correction algorithm.

Measurements from the operational surface drifting and fixed buoy programs will be used to characterize the surface temperature fields and to validate the atmospheric

correction algorithms used with data from the AVHRR (Advanced Very High Resolution Radiometer) as in the fashion developed for the AVHRR SST Pathfinder program.

The assimilated meteorological fields produced by operational weather services (National Meteorological Center, European Centre for Medium-Range Weather Forecasting) provide a valuable description of the marine atmosphere and surface (strictly sub-surface bulk) sea temperature. These fields will be used in conjunction with the radiative transfer modeling to simulate the MODIS measurements, initially to give confidence that the selection of radiosoundings used to characterize the marine atmosphere is indeed representative, and, subsequently, if it can be shown that the assimilated fields are of sufficiently high accuracy, to provide direct input to the radiative transfer modeling.

4.3.3 Existing satellite data

Measurements from the AVHRR and ATSR (Along Track Scanning Radiometer) on the ERS satellites [Edwards *et al.*, 1990; Minnett, 1995a & 1995b] will be used in the pre-launch phase to study the error characteristics of their SST fields [e.g. Podestá, *et al.*, 1997]. The long wave channels of both of these instrument types match quite well the spectral characteristics of the MODIS long-wave channels (31 and 32), and the noise characteristics of the ATSR channels are very good (see 4.3 below). The ATSR series are radiometers that are very well characterized before launch and have two internal black-body targets for in-flight calibration [Armitage *et al.*, 1990; Minnett 1985b]. Both AVHRR and ATSR have single channels in the 3.5 - 4.0 μm window and so cannot supply comparable data to those expected from MODIS channels 20, 22 and 23.

4.4 Post-launch activities

The initial post-launch activities will focus on gathering surface and atmospheric data that are collocated and contemporaneous with the MODIS measurements.

4.4.1 Planned field activities and studies

It is anticipated that the initial validation campaigns will be centered on the DOE ARM sites in the TWP and the NSA-AOO where the instrumentation installed there will provide an unparalleled description of the state of the atmosphere. As part of the ARM operations periodic Intensive Operations Periods [Stokes and Schwartz, 1994] are

undertaken during which the sampling frequency and is increased and additional, often experimental instruments, are deployed. Particular attention will be paid to the possibility of coordinating MODIS validation with ARM activities during these periods.

Cruises of opportunity, such as those associated with the MOBY and the possible supplementary ARM ocean sites, will be exploited wherever possible. Another exciting possibility would be to mount an M-AERI on one of the Antarctic research support vessels on one of more of their transoceanic cruises to Antarctica. US Coast Guard ice-breakers sail from Seattle to Antarctica each year, and an ice-strengthened research ship of the British Antarctic Survey makes comparable voyages in the Atlantic Ocean. In addition, it is anticipated that the M-AERI will be deployed on fixed research platforms during this period.

Low-flying aircraft provide alternative platforms for the validating radiometers, and aircraft can seek out the clear air conditions, avoiding the clouds that obscure the position of fixed or slowly moving ships at the times of satellite overpasses on a significant number of occasions. Collaborations will be forged with groups using HIS-type instruments on aircraft that can fly low ($h < 50\text{m}$) over the ocean.

Broad band infrared radiometers, if proven to be beneficial during the pre-launch studies, will be used on ships of opportunity as these arise.

In collaboration with the MODIS Atmospheric group, high-flying aircraft campaigns will be utilized, when their planned flights include segments over the ocean.

Comparisons between MODIS SST fields and measurements from analysis of fixed and drifting surface buoys will be continued throughout the MODIS missions to provide long-term monitoring of the performance of the SST algorithm and data for progressive algorithm refinement. This is dealt with in more detail in section 5.

4.4.2 New-EOS Targeted coordinated field campaigns

Several aircraft campaigns of the MODIS Atmospheric Group are planned to be made over mid-latitude oceanic areas in the first few years of MODIS operations. These will be used to validate the MODIS top-of-atmosphere radiance measurements and SST retrievals. At present it is not clear what research cruises will be being undertaken in

the post-launch period, but efforts will be made to coordinate MODIS infrared validation exercises with those that offer promising opportunities.

4.4.3 Needs for other satellite data

Inter-satellite comparisons can be done on an opportunistic basis throughout the mission, provided suitable validating instruments are flying on other satellites. In the period of the first few years of the of the AM-1 mission, possible validating instruments are the Advanced Very High Resolution Radiometer on the NOAA satellites, the Along-Track Scanning Radiometer (ATSR) on the ERS-2 satellite, or the Advanced ATSR on the European Polar Platform of the Envisat-1 Mission, scheduled for launch in mid - 1999 [Cendral, 1995], the Ocean Color and Temperature Scanner (OCTS) on the Japanese ADEOS satellite launched in 1996, and the Global Imager (GLI) on the (ADEOS-II) satellite. All of these instruments have a spatial resolution of 1km at nadir, with the exception of OCTS, which has a spatial resolution of 0.7km. The infrared channelization and noise characteristics for the MODIS, AVHRR, ATSR, OCTS and GLI instruments are given in the following table.

Table 2. Channel characteristics of satellite-borne infrared radiometers

| | MODIS ¹ | | AVHRR ² | | ATSR ³ | | OCTS ⁴ | | GLI ⁵ | |
|-----|-----------------------------|-------------------|-----------------------------|-------------------|-----------------------------|-------------------|-----------------------------|-------------------|-----------------------------|-------------------|
| NO. | λ (μm) | NE Δ T (K) | λ (μm) | NE Δ T (K) | λ (μm) | NE Δ T (K) | λ (μm) | NE Δ T (K) | λ (μm) | NE Δ T (K) |
| 20 | 3.75 | 0.05 | 3.75 | 0.1 2 | 3.7 | 0.019 | 3.7 | 0.15 | 3.715 | <0.15 |
| 22 | 3.96 | 0.05 | | | | | | | | |
| 23 | 4.05 | 0.05 | | | | | | | | |
| 29 | 8.55 | 0.05 | | | | | 8.52 | 0.15 | 8.3 | <0.1 |
| 31 | 11.03 | 0.04 | 10.5 | 0.1 2 | 10.8 | 0.028 | 10.8 | 0.15 | 10.8 | <0.1 |
| 32 | 12.02 | 0.04 | 11.5 | 0.1 2 | 12. | 0.025 | 11.9 | 0.15 | 12 | <0.1 |

¹ For Proto-Flight Model. From graphic presented by T. Pagano at MODIS Science Team Meeting, November 1995.

² For a target temperature of 300K. From Planet, 1988.

³ Derived from 500 samples of black-body measurement at a temperature of 298K. [From Minnett, 1995b].

⁴ For a target temperature of 300K. From OCTS instrument description.

⁵ From NASDA Research Announcement , October 24, 1995.

4.4.4 Measurement needs (*in situ*) at calibration/validation sites

Validation sites will be selected where the ancillary measurements needed to specify the atmospheric state, such as at the ARM sites (see above). At this stage it is not possible to foresee whether the instrumentation suites at these site will need augmentation. If broad-band infrared radiometers can be shown to provide SST measurements of sufficient reliability to validate the MODIS retrievals, and if these are deployed on ships of opportunity, it may be necessary to augment the instruments on these ships to provide the necessary ancillary measurements, such as radiosondes and a sky camera. Similarly, when the M-AERI is deployed on fixed platforms, it is likely that additional instruments will be needed to provide the atmospheric measurements.

The spatial distribution of the set of the operational free-drifting buoys may not be ideal for the long-term validation of the MODIS SST retrievals, in which case it will be necessary to seed particular ocean areas that are critical to the validation, but are inadequately sampled by the buoys in place at that time.

4.4.5 Needs for instrument development

The continuing development of the M-AERI is anticipated to provide a reliable and accurate primary validation instrument by the time of the MODIS launch. If the deployment of broad-band infrared radiometers on a larger number of ships of opportunity is found to be desirable from the pre-launch studies, it may be necessary to develop improvements on the commercially available models, such as *in situ* calibration equipment to improve the long-term stability and accuracy of the measurements.

4.4.6 Geometric registration site

It is not anticipated that such a facility will be needed for the MODIS infrared channel validation over the oceans.

4.4.7 Intercomparisons (Multi-instrument)

Intercomparison with other satellite instruments will be primarily with instruments on other platforms (see 4.3.3 and 4.4.3). Comparisons are planned with the ASTER instruments to use their high spatial resolution to explore the influences of sub-pixel

features, such as small clouds, or the MODIS Sea-Surface temperature retrievals. The MODIS aerosol products, derived by the Ocean Color Group (Howard Gordon) and the Atmospheric Group (Yoram Kaufman, Didier Tanré) are expected to be of use in determining the causes of the residual errors in the MODIS SST retrievals.

4.5 Implementation of validation results in data production

4.5.1 Approach

The algorithm for SST derivation from the MODIS infrared measurements will be supplied before launch. To provide a consistent output data stream, it is important that the data production algorithm not be adjusted frequently, and when it is revised the changes must be well recorded in the metadata associated with the product. It is anticipated that for the first 12-24 months after launch, the validation data will be analyzed in a ‘research’ mode and trial refinements of the algorithm will be fully tested off-line before being implemented at the processing center. It is expected that part of the algorithm refinement will incorporate findings and results from other groups, especially those that are also involved in monitoring the on-board infrared calibration process. Retrospective reprocessing of data will be done on large data segments, say of a year’s length or more, at which time it will be necessary to distribute the revised products to all users of the previous product versions.

4.5.2 Role of EOSDIS

EOSDIS will be a valuable source of existing data and analysis tools to be used in the pre-launch algorithm development and in the post-launch validation activities. EOSDIS will be responsible for providing all operational products used in the validation program.

4.5.3 Plans for archival of validation data

All data sets gathered or derived for the purposes of validation of the MODIS infrared channels will be made available to the scientific community through EOSDIS and the World Wide Web.

5.0 Validation using *in situ* sea surface temperature measurements

Section 4 dealt with the radiometric aspects of validating the MODIS infrared measurements over the areas. This section deals with validation activities using long time series of *in situ* sea surface temperatures derived from surface buoys. This activity builds on the experience gained in the NASA/NOAA AVHRR Ocean Pathfinder project, and will be conducted in close collaboration with the MODIS activities being led by Dr. R.H. Evans of the Rosenstiel School of Marine and Atmospheric Science.

We will characterize overall algorithm performance by assembling two comparison databases: a North American match-up database (MDB) and a Global match-up database. The North American MDB will be principally composed of surface observing sites in North American coastal waters while the global MDB will include all fixed and drifting platforms. Data availability drives generation of the two comparison datasets. Currently the North American observations are available in near real time while the global observations have delays of days to weeks associated with their retrieval.

5.1 Sources of *in situ* SSTs and other environmental variables

The environmental data used in both MDBs will be obtained from the various sources summarized in Table 2. The observations are from two main types of platforms: moored buoys and drifting buoys. The North American MDB will contain *in situ* observations only from the US National Data Buoy Center (NDBC) moored buoys located from the Gulf of Maine to the Gulf of Mexico (latitudinal range: 42.5°N to 25.9°N).

Table 3. Sources of *in situ* SST Values to be Included in the MODIS Sea_sfc Temperature Algorithm Matchup Databases

| TYPE | PLATFORM | SOURCE |
|----------------|----------|--|
| Moored buoys | NDBC | US National Data Buoy Center, NDBC (via NASA/GSFC) |
| | Japanese | Japanese Meteorological Agency |
| | TOGA/TAO | NOAA Pacific Meteorological and Environmental Laboratory |
| Drifting Buoys | AOML | NOAA Atlantic Oceanographic and Meteorological Laboratory |
| | MEDS | Canadian Marine Environmental Data Service (via NASA/GSFC) |

Some of the *in situ* platforms (particularly the moored buoys) include environmental variables other than SST. The version of the Global MDB, however, will include only the following *in situ* quantities, which are common to all data sources:

- Buoy ID
- Latitude
- Longitude
- Time
- Sea surface temperature

On the other hand, the North American MDB will include the following additional environmental variables:

- Significant wave height
- Air temperature
- Wind speed and direction (average over the first 8 minutes of each reporting period, usually once per hour)
- Dew point temperature

5.2 MODIS Data Extractions

For both the MDBs, MODIS data will be extracted for 3x3-pixel boxes centered at each *in situ* SST location. The initial extraction data set includes only the level 1a counts, which are converted to brightness temperature in a subsequent step. We assume a navigation correction (time and attitude) is applied to ensure correct geolocation of the satellite data.

The MDBs will include coefficients that can be used to correct the various IR channels for changes in emissivity as a function of scan angle (variables em_j ; see below for location in the record). These coefficients are taken from Bransom [1968] but new values derived from M-AERI measurements will be used if necessary. Emissivity-corrected values for the central pixel are also included in the MDB for the various channels (cm_i). Note that since the correction is performed on radiances, one cannot simply multiply the uncorrected temperatures by the coefficients and obtain the corrected values.

5.2.1 Time Coordinates

To facilitate the matchup process, dates and times of both the satellite and *in situ* data will be converted to a continuous time coordinate, *e.g.*, “seconds since January 1, 1981” is used in the Pathfinder analog. These values can be subtracted and then the actual date can be obtained through simple calculation.

5.3 Matchup Procedures

The *in situ* records are first temporally matched-up against the MODIS extractions. To limit variability introduced by the time separation between the two data sources, the absolute difference between the time of the *in situ* SST measurement and the time at which that location is viewed by the MODIS (*i.e.*, the matchup time window) is restricted to a maximum of ± 30 minutes or ± 15 minutes. *In situ* records that do not fall within the stipulated time window will be rejected.

The *in situ* records that pass the temporal matchup subsequently have to pass a spatial test. A maximum distance of 0.1° will be accepted between an *in situ* SST location and the location of the central pixel in the MODIS extraction box.

5.3.1 Filtering Records

To reduce the number of records to be handled by users of the databases, the matchups will be passed through a series of filters that eliminate records with obvious problems (for instance, gross cloud contamination). The records will be included in the MDB files only if they pass the following series of tests (the variable names used in the tests are described in Tables 4 and 5):

Table 4. Fields included in global matchup database (version 1).

| Field No. | Field Description | Units | Code |
|-----------|--|---------|-------|
| 1 | Satellite observation time | Seconds | stime |
| 2 | Latitude of center pixel | Degrees | slat |
| 3 | Longitude of center pixel | Degrees | slon |
| 4 | Average PRT temperature | °C | prt |
| 5 | Solar zenith angle | Degrees | solz |
| 6 | Satellite zenith angle | Degrees | satz |
| 7 | Glint index | — | glnt |
| 8 | Emmisivity correction, channel 20/22/23 | — | em20 |
| 9 | Emmisivity correction, channel 31 | — | em31 |
| 10 | Emmisivity correction, channel 32 | — | em32 |
| 11 | Central value of 3x3 pixel box, channel 20 | °C | ch20 |
| 12 | Central value of 3x3 pixel box, channel 22 | °C | ch22 |
| 13 | Central value of 3x3 pixel box, channel 23 | °C | ch23 |
| 14 | Central value of 3x3 pixel box, channel 31 | °C | ch31 |
| 15 | Central value of 3x3 pixel box, channel 32 | °C | ch32 |
| 16 | Median of 3x3 pixel box, channel 20 | °C | med20 |
| 17 | Median of 3x3 pixel box, channel 22 | °C | med22 |
| 18 | Median of 3x3 pixel box, channel 23 | °C | med23 |
| 19 | Median of 3x3 pixel box, channel 31 | °C | med31 |
| 20 | Median of 3x3 pixel box, channel 32 | °C | med32 |
| 21 | Minimum value of 3x3 pixel box, channel 20 | °C | min20 |
| 22 | Minimum value of 3x3 pixel box, channel 22 | °C | min22 |
| 23 | Minimum value of 3x3 pixel box, channel 23 | °C | min23 |
| 24 | Minimum value of 3x3 pixel box, channel 31 | °C | min31 |
| 25 | Minimum value of 3x3 pixel box, channel 32 | °C | min32 |
| 26 | Maximum value of 3x3 pixel box, channel 20 | °C | max20 |
| 27 | Maximum value of 3x3 pixel box, channel 22 | °C | max22 |
| 28 | Maximum value of 3x3 pixel box, channel 23 | °C | max23 |
| 29 | Maximum value of 3x3 pixel box, channel 31 | °C | max31 |
| 30 | Maximum value of 3x3 pixel box, channel 32 | °C | max32 |
| 31 | Average value of 3x3 pixel box, channel 20 | °C | av20 |
| 32 | Average value of 3x3 pixel box, channel 22 | °C | av22 |
| 33 | Average value of 3x3 pixel box, channel 23 | °C | av23 |
| 34 | Average value of 3x3 pixel box, channel 31 | °C | av31 |
| 35 | Average value of 3x3 pixel box, channel 32 | °C | av32 |
| 36 | PRT 1 Temperature) | °C | prt1 |
| 37 | PRT 2 Temperature) | °C | prt2 |
| 38 | PRT 3 Temperature) Black body monitor | °C | prt3 |
| 39 | PRT 4 Temperature) | °C | prt4 |
| 40 | Central value w/ emmisivity correction, channel 20 | °C | cm20 |
| 41 | Central value w/ emmisivity correction, channel 22 | °C | cm22 |
| 42 | Central value w/ emmisivity correction, channel 23 | °C | cm23 |
| 43 | Central value w/ emmisivity correction, channel 31 | °C | cm31 |
| 44 | Central value w/ emmisivity correction, channel 32 | °C | cm32 |
| 45 | Time of <i>in situ</i> observation | Seconds | btime |
| 46 | Buoy latitude | Degrees | blat |
| 47 | Buoy longitude | Degrees | blon |
| 48 | Buoy ID | — | bid |
| 49 | <i>In situ</i> SST | °C | bsst |
| 50 | Delta-SST (First-guess satellite SST minus <i>in situ</i> SST) | °C | sst1 |
| 51 | Filter code (1 or 2) | — | pass |

Table 5. Fields included in North American matchup database (version 1).

| Field No. | Field Description | Units | Code |
|-----------|--|---------|-------|
| 1 | Satellite observation time | Seconds | stime |
| 2 | Latitude of center pixel | Degrees | slat |
| 3 | Longitude of center pixel | Degrees | slon |
| 4 | Average PRT temperature | °C | prt |
| 5 | Solar zenith angle | Degrees | solz |
| 6 | Satellite zenith angle | Degrees | satz |
| 7 | Glint index | — | glnt |
| 8 | Emmisivity correction, channel 20, 22, 23 | — | em20 |
| 9 | Emmisivity correction, channel 31 | — | em31 |
| 10 | Emmisivity correction, channel 32 | — | em32 |
| 11 | Central value of 3x3 pixel box, channel 20 | °C | ch20 |
| 12 | Central value of 3x3 pixel box, channel 22 | °C | ch22 |
| 13 | Central value of 3x3 pixel box, channel 23 | °C | ch23 |
| 14 | Central value of 3x3 pixel box, channel 31 | °C | ch31 |
| 15 | Central value of 3x3 pixel box, channel 32 | °C | ch32 |
| 16 | Median of 3x3 pixel box, channel 20 | °C | med20 |
| 17 | Median of 3x3 pixel box, channel 22 | °C | med22 |
| 18 | Median of 3x3 pixel box, channel 23 | °C | med23 |
| 19 | Median of 3x3 pixel box, channel 31 | °C | med31 |
| 20 | Median of 3x3 pixel box, channel 32 | °C | med32 |
| 21 | Minimum value of 3x3 pixel box, channel 20 | °C | min20 |
| 22 | Minimum value of 3x3 pixel box, channel 22 | °C | min22 |
| 23 | Minimum value of 3x3 pixel box, channel 23 | °C | min23 |
| 24 | Minimum value of 3x3 pixel box, channel 31 | °C | min31 |
| 25 | Minimum value of 3x3 pixel box, channel 32 | °C | min32 |
| 26 | Maximum value of 3x3 pixel box, channel 20 | °C | max20 |
| 27 | Maximum value of 3x3 pixel box, channel 22 | °C | max22 |
| 28 | Maximum value of 3x3 pixel box, channel 23 | °C | max23 |
| 29 | Maximum value of 3x3 pixel box, channel 31 | °C | max31 |
| 30 | Maximum value of 3x3 pixel box, channel 32 | °C | max32 |
| 31 | Average value of 3x3 pixel box, channel 20 | °C | av20 |
| 32 | Average value of 3x3 pixel box, channel 22 | °C | av22 |
| 33 | Average value of 3x3 pixel box, channel 23 | °C | av23 |
| 34 | Average value of 3x3 pixel box, channel 31 | °C | av31 |
| 35 | Average value of 3x3 pixel box, channel 32 | °C | av32 |
| 36 | PRT 1 Temperature) | °C | prt1 |
| 37 | PRT 2 Temperature) | °C | prt2 |
| 38 | PRT 3 Temperature) Black body monitor | °C | prt3 |
| 39 | PRT 4 Temperature) | °C | prt4 |
| 40 | Central value w/ emmisivity correction, channel 20 | °C | cm20 |
| 41 | Central value w/ emmisivity correction, channel 22 | °C | cm22 |
| 42 | Central value w/ emmisivity correction, channel 23 | °C | cm23 |
| 43 | Central value w/ emmisivity correction, channel 31 | °C | cm31 |
| 44 | Central value w/ emmisivity correction, channel32 | °C | cm32 |
| 45 | Delta-SST (First-guess satellite SST minus <i>in situ</i> SST) | °C | sst1 |
| 46 | Filter code (1 or 2) | — | pass |
| 47 | Time of <i>in situ</i> observation | Seconds | btime |
| 48 | Buoy latitude | Degrees | blat |
| 49 | Buoy longitude | Degrees | blon |
| 50 | Buoy ID | — | bid |
| 51 | Buoy air temperature | °C | bat |
| 52 | Buoy dew point temperature | °C | bdwp |
| 53 | Buoy wind speed | m/s | bwsp |
| 54 | Buoy wind direction | Degrees | bwdir |
| 55 | Buoy significant wave height | m | bswh |
| 56 | Buoy sea surface temperature | °C | bsst |

- Bsst (Buoy SST) ne “n/a”
- Ch31 (brightness temperature) < 35°C
- Ch32 (brightness temperature) < 35°C
- Satz (satellite zenith angle) < 62°

- $\text{Cen20 (field 13) - Cen32 (field 15)} < 6^{\circ}\text{C}$ and
 $\text{Cen20 (field 13) - Cen32 (field 15)} > -2^{\circ}\text{C}$
- $(\text{Max31} - \text{Min31}) \leq 3^{\circ}\text{C}$ and
 $(\text{Max32} - \text{Min32}) \leq 3^{\circ}\text{C}$

A second set of tests define two categories for a “pass” index, which can serve as an initial guidance for data selection:

- If $1^{\circ}\text{C} \leq (\text{Max31} - \text{Min31}) < 3^{\circ}\text{C}$ and $1^{\circ}\text{C} \leq (\text{Max32} - \text{Min32}) < 3^{\circ}\text{C}$, then pass = 2
- If $(\text{Max31} - \text{Min31}) < 1^{\circ}\text{C}$ and $(\text{Max32} - \text{Min32}) < 1^{\circ}\text{C}$, then pass = 1.

The general approach is that the more restrictive criteria for the spatial homogeneity tests (*i.e.*, records with pass=1) can be used to estimate SST algorithm coefficients. The records with pass=2 can be used in evaluating algorithm performance. The “pass” code is included as the last field of the matchup record.

5.3.2 First-guess satellite-derived SST

As a further aid to initial use of the matchup data sets, a first-guess satellite SST (sst1) will be computed. The difference between this first-guess satellite SST and the *in situ* SST will be included in the MDBs. The first-guess SST will be computed using an MCSST. [The matchup databases will not actually include the first-guess satellite SST (sst1), but the difference between sst1 and the *in situ* SST.]

5.4 Matchup database definition

The matchup database files will be maintained as flat ASCII files, with free-format blank-separated fields in each record. The number of fields per record is 51 for the Global MDB and 56 for the North American MDB. Missing values are denoted by “n/a”. The fields included in both types of MDBs vary somewhat, as does their location in the record. The variables included in the global and the experimental MDBs are listed in Tables 3 and 4, respectively.

The first record in all the MDB files should be a header containing blank-separated short field names to be used if the records are imported into a spreadsheet or statistical

package; these short names or codes are shown on the fourth columns of Tables 3 and 4. Specific details for each MDB type are given in Tables 3 and 4.

5.5 Quality Control and Diagnostics

Quality control of the MODIS Sea_sfc Temperature algorithm fields is not necessarily easy since there currently do not exist any other sea surface temperature fields with similar spatial and temporal coverage. The only current candidate fields with requisite accuracy and coverage are the experimental ERS-1 Along Track Scanning Radiometer (ATSR) and the NOAA-NASA Pathfinder SST fields. While these fields have great potential for retrospective studies of MODIS Sea_sfc Temperature algorithm performance, they do not address the need for near-real time quality assessment of the product. Thus we propose four methods: 1) a running climatology computed from the product itself, 2) a lower resolution SST estimate computed from the AIRS instrument (product 2523), 3) comparisons with NOAA and NAVY SST products, and 4) space-time coherence tests.

5.5.1 Running Climatology Approach

An approach which has been shown to be effective in the NOAA/NASA AVHRR Pathfinder work is to compute a lagged climatology of the global SST where the lag (time) interval might be one week, two weeks, or a month. This running Global average temperature field is used at high resolution to provide first guess temperature for all pixel locations. The running climatology includes a mean value and a variance field for each location, T_c and V_c , respectively. T_c and V_c are functionals of space and time, *i.e.*, $T_c = T_c(x,y,t)$ and $V_c = V_c(x,y,t)$. A range measure is adopted to classify data outliers. For example, the Global range measure might be $\pm 2\sigma$ (units of standard deviation). Data which lies within two standard deviations of T_c would be considered as a valid estimate, that is

$$\boxed{(T_c - 2\sqrt{V_c}) \leq T_s \leq (T_c + 2\sqrt{V_c})} \quad (20)$$

Maintenance of such a climatology for the MODIS SST algorithm has computing and mass storage implications. Each observing day a new climatology will be computed over the lag interval. Testing with the NOAA/NASA Pathfinder activity has demonstrated that one should keep separate day/night climatologies due to daytime

skin – bulk T_s biases. Therefore, the climatology requires producing an average value and a variance for the last n days of each field every day and storing this for quality assessment use. Each field will have the characteristics shown in Table 6.

Table 6. MODIS IR SST Climatology Dataset

| Parameter | Format |
|-------------------|-----------------------|
| Average SST value | 32 bit floating point |
| Variance estimate | 32 bit floating point |
| Latitude | 32 bit floating point |
| Longitude | 32 bit floating point |
| Time | 32 bit floating point |

Given the data structure shown in Table 5, each day/night climatology field will require approximately 7.5 Gbytes per day, or a total of 15 Gbytes per day (3.5×10^8 (ocean pixels) \times 20 bytes/pixel \times 2 fields/day, or ~ 15 Gbytes/day).

5.5.2 Space/time Coherence

The previously mentioned quality assessment approaches rely on the presence of global fields for their implementation. Oceanographers typically test new observing systems by looking at sections in space or time, *i.e.*, time, space, or space/time series.

As part of the ongoing quality assessment activity, we will define a sequence of points for the production of time series, several space cuts through better *in situ* observed regions of oceanic basins, and a few specific sections for the generation of space/time diagrams. Products from this activity will facilitate quick look tests of space/time coherence.

5.6 Implications for the ECS, TLCF and MOTCF Efforts

It is unclear which facilities will generate the climatology and other quality control products. It is apparent they can be generated in the ECS or by the TLCF or by the MOTCF. We note that one of them will have to produce the various products on a routine basis.

5.7 Exception Handling

Exception handling for the Sea_sfc Temperature algorithm is straightforward. To our knowledge there is no processing condition which should 'hold' Sea_sfc temperature processing. Data quality flags will be provided for all anomalous cases. The approach is to process all available non-land infrared radiances for Sea_sfc temperature, and then flag each estimate for missing radiances, clouds, dropouts, *etc.* As is stated in the calibration-validation section, we require daily day / night global mosaics of the Sea_sfc Temperature, flag words, with compilations of numbers of each flag's occurrence. Note: clouds are a special case - we use the results of product 3660 as one way to mark cloudy pixels.

5.8 Data Dependencies

Data dependencies for the MODIS Sea_sfc Temperature proto-algorithm are as follows. This product itself requires Level-1A infrared radiances (product 3708) for bands 20, 22, 23, 31 and 32, and the cloud screening (product 3660). Visible and near infrared radiances (bands 3,4,5,6) will be used as a secondary cloud flag in the event that the cloud screening product is not available. Future versions of this algorithm may use surface wind estimates to better determine the extent of sun-glint and skin- *vs.* bulk-temperature differences during daytime passes. The AIRS SST estimate (product 2523) will be used in near-real time quality assessment of skin temperature. Data dependencies are specified in Table 6. Note that the only products which must be available for Sea_sfc product generation are the Level 1A Radiances (product 3708) and the cloud screening (product 3660).

Table 7. MODIS Sea_sfc Data Dependencies

| Instrument | Product | Product # | Band | Necessary |
|------------|-------------------|-----------|-------------------------|-----------|
| MODIS | Level 1A Radiance | 3708 | 3,4,5,6,20,22,23,31,32* | Yes |
| Various | Cloud Screening | 3660 | n/a | Yes |
| NSCATT-II | Sigma 0 | 3721 | n/a | No |
| AIRS | SST (Skin) | 2523 | n/a | No |

* Note: Bands 3,4,5,6 are averaged to 1000 m IFOV.

5.9 Output Product

Output retrieved SST estimates for the MODIS Sea_sfc Temperature algorithm are vectors composed of the retrieved SST value, input calibrated radiances, and derived brightness temperatures for each channel, flags which quantify the cloud screening results, latitude, longitude and time. There are two products: a quality assessment product for internal use (Table 8) and the Sea_sfc temperature product for external use (Table 9). A description of the vector components and data types is given in Tables 8 and 9.

Table 8. MODIS IR SST Quality Assessment Product

| Parameter | Format |
|------------------------------------|-----------------------|
| SST estimate | 32 bit floating point |
| Latitude | 32 bit floating point |
| Longitude | 32 bit floating point |
| Time | 32 bit floating point |
| Satellite Zenith Angle | 32 bit floating point |
| Solar Zenith Angle | 32 bit floating point |
| Calibrated Radiance - Channel 1 | 32 bit floating point |
| ... | 32 bit floating point |
| Calibrated Radiance - Channel n | 32 bit floating point |
| Brightness Temperature - Channel 1 | 32 bit floating point |
| ... | 32 bit floating point |
| Brightness Temperature - Channel n | 32 bit floating point |
| Quality Control Flags - 1 | 16 bit integer |
| Quality Control Flags - 2 | 16 bit integer |

Table 9. MODIS IR SST Output Product 2527

| Parameter | Format |
|---------------------------|-----------------------|
| SST estimate | 32 bit floating point |
| Latitude | 32 bit floating point |
| Longitude | 32 bit floating point |
| Time | 32 bit floating point |
| Quality Control Flags - 1 | 16 bit integer |
| Quality Control Flags - 2 | 16 bit integer |

These tables provide a basis for estimation of the output data flow for the algorithm. The level 2 output product has a data flow of 3.5×10^8 (ocean pixels) \times 20 bytes/pixel \times 2 fields/day or ~15 Gbytes/day. The data assessment product has a data flow of 3.5×10^8 (ocean pixels) \times 84 bytes/pixel \times 2 fields/day or ~63 Gbytes/day.

6.0 Constraints, Limitations, Assumptions

Major constraints on data quality outside the scope of this effort focus in the following areas: accurate pre-launch instrument characterization, instrument NE Δ T for each channel, calibration model performance, availability of quality controlled surface calibration-validation observations, availability and access to the various quality assessment data sets, and timely access to continuing performance assessment data sets. The on-orbit instrument NE Δ T performance is a primary input to the algorithm error budget. Similarly, a robust calibration model which minimizes radiometer calibration inaccuracies is a necessary requirement for good algorithm performance - this model must limit the non-linear components of such inaccuracies to the least bit count. Surface calibration/validation is also necessary to maintain a regular series of comparison observations to demonstrate system performance. Combination of the surface calibration/validation observations with the quality assessment datasets will permit documentation of system performance and addressing of any anomalies in a timely manner.

7.0 References

- Abbott, M.R. and D.B. Chelton, 1991. Advances in passive remote sensing of the ocean. US National Report to IUGG. *Rev. of Geophys., Supplement*: 571-583.
- Armitage, S., D. Corney, G. Mason, W. H. Taylor, R. E. J. Watkins, E. J. Williamson, D. Cragg, G. Mellor, D. Tinkler, A. R. Holmes, W. Linford and F. Spry, 1990. Test and calibration of the Along Track Scanning Radiometer (ATSR). Proceedings of the International Symposium on Environmental Testing for Space Programmes - Test, Facilities and Methods. ESA SP-304. 559.
- Anding, D. and R. Kauth, 1970. Estimation of Sea Surface Temperature from Space. *Remote Sensing of the Environment* **1**, 217-220.
- Barton, I.J., A.J. Prata, and D.T. Llewellyn-Jones, 1993. The Along Track Scanning Radiometer—an Analysis of coincident ship and satellite measurements, *Adv. Space Res.*, **13(5)**, 69.

- Barton, I.J., M. Zavody, D.M. O'Brien, D.R. Cutten, R.W. Saunders and D.T. Llewellyn-Jones, 1989. Theoretical algorithms for satellite-derived sea surface temperatures. *J. Geophys. Res.*, **94**, 3365.
- Bradshaw, J.T., H.E. Fuelberg, 1993: An evaluation of HIS interferometer soundings and their use in mesoscale analysis. *J. Appl. Meteor.*, **32**, 522-538.
- Bransom, M.A., 1968). *Infrared radiation*, New York, Plenum Press, 623 pp.
- Brown, O.B. and R.E. Cheney, 1983. Advances in satellite oceanography. *Rev. Geophys. and Space Phys.*, **21**(5), 1216-1230.
- Brown, O.B., J. W. Brown and R.H. Evans, 1985. Calibration of advanced very high resolution radiometer infrared observations. *J. Geophys. Res.*, **90**(C6): 11667-11677.
- Cendral, C.J. 1995. Polar Platform for Envisat-1 mission. *Earth Observation Quarterly*, no **49**, p16.
- Chahine, M.T., 1980. Infrared remote sensing of sea surface temperature. In *Remote Sensing of Atmospheres and Oceans*, ed. A. Deepak, Academic Press, New York, pp. 411-434.
- Cornillon, P., and L. Stramma, 1985. The distribution of diurnal sea surface warming events in the western Sargasso Sea. *J. Geophys. Res.*, **98**(C6), 11811-11815.
- Deschamps, P.Y. and T. Phulpin, 1980. Atmospheric corrections of infrared measurements of sea surface temperature using channels at 3.7 μm , 11 μm and 12 μm . *Boundary Layer Meteor.* **18**, 131-143.
- Edwards, T., R. Browning, J. Delderfield, D. J. Lee, K. A. Lidiard, R. S. Milborrow, P. H. McPherson, S. C. Peskett, G. M. Toplis, H. S. Taylor, I. Mason, G. Mason, A. Smith and S. Stringer, 1990. The Along Track Scanning Radiometer - Measurement of sea-surface temperature from ERS-1. *Journal of the British Interplanetary Society*, **43**, 160.
- ESSC, 1988. *Earth System Science: A Closer View*. Report of the Earth System Sciences Committee, NASA Advisory Council. Available from Office for Interdisciplinary Earth Studies, University Corporation for Atmospheric Research, Boulder, CO, 208 pp.
- GOFS, 1984. *Global Ocean Flux Study, Proceedings of a Workshop, September 10-14, 1984*. National Academy of Sciences Press, Washington, D.C., 360 pp.
- King, M., and D. Herring, 1992. The MODIS Airborne Simulator (MAS). *The Earth Observer*, Nov/Dec 1992.

- Lauritson, L., G.J. Nelson and F.W. Porto, 1979. Data extraction and calibration of TIROS-N/NOAA radiometers. NOAA TM NESS 107. US Government Printing Office, Washington, D.C., 81 pp. Available from NTIS.
- Llewellyn-Jones, D.T., P.J. Minnett, R.W. Saunders and A.M. Zavody, 1984. Satellite multichannel infrared measurements of sea surface temperature of the N.E. Atlantic Ocean using AVHRR/2. *Quart. J. R. Met. Soc.* **110**, 613-631.
- McClain, E.P., 1981. Multiple atmospheric -- window techniques for satellite derived sea surface temperatures. *Oceanography from Space*, **13**, J.F.R. Gower, ed., Plenum, New York.
- McClain, E.P., W.G. Pichel, C.C. Walton, Z. Ahmed, and J. Sutton, 1983. Multi-channel improvements to satellite derived global sea surface temperatures. Proc. XXIV COSPAR, *Advances Space Res.* **2**(6), 43-47.
- McClain, E.P., W.G. Pichel and C.C. Walton, 1985. Comparative performance of AVHRR-based multichannel sea surface temperatures. *J. Geophys. Res.* **90**(C6), 11587-11601.
- Minnett, P.J., 1986. A numerical study of the effects of anomalous North Atlantic atmospheric conditions on the infrared measurement of sea surface temperature from space. *J. Geophys. Res.*, **91**(C7), 8509-8521.
- Minnett, P.J., 1990a. Satellite infrared scanning radiometers - AVHRR & ATSR. In *Microwave Remote Sensing for Oceanographic and Marine Weather-Forecast Models*, R.A. Vaughn, ed. Kluwer Academic Publishers.
- Minnett, P.J., 1990b. The regional optimization of infrared measurements of sea-surface temperature from space. *J. Geophys. Res.*, **95**, 13,497-13,510.
- Minnett, P.J., 1991. Consequences of sea surface temperature variability on the validation and applications of satellite measurements. *J. Geophys. Res.*, **96**, 18,475-18,489.
- Minnett, P.J., 1995a. Sea surface temperature measurements from the Along-Track Scanning Radiometer on ERS-1. In "Oceanographic Applications of Remote Sensing", M. Ikeda and F. Dobson (eds.). CRC Press Inc. 131-143.
- Minnett, P.J., 1995b. The Along-Track Scanning Radiometer: Instrument Details. In "Oceanographic Applications of Remote Sensing", M. Ikeda and F. Dobson (eds.). CRC Press Inc. 461-472.
- MODIS, 1986. *MODIS, Moderate-resolution imaging spectrometer, Earth Observing System, IIb*. Instrument Panel Report, National Aeronautics and Space Administration, Washington, D.C., 59 pp.

- Nalli, N.R., 1995. Sea surface skin temperature retrieval using the High-Resolution Interferometer Sounder, MS Thesis, University of Wisconsin-Madison. 117pp.
- Planet, W. (Ed). Data extraction and calibration of TIROS-N/NOAA radiometers. NOAA Tech. Memo. NESS 107- Rev.1. October, 1988.
- Podestà, G.P., S.C. Shenoi, J.W. Brown and R.H. Evans, 1990. AVHRR Pathfinder Oceans Matchup database 1985-1994 (Version 18).
- Podestà, G.P., S.C. Shenoi, R.H. Evans and O.B. Brown, 1997. Paper in preparation.
- Prabhakara, C., G. Dalu and V.G. Kunde, 1974. Estimation of Sea Surface Temperature from remote sensing in the 11 μm to 13 μm window region. *J. Geophys. Res.* **79**(12), 1744-1749.
- Robinson, I.S., Wells, N.C. and Charnock, H. 1984. The sea surface thermal boundary layers and its relevance to the measurement of sea surface temperature by airborne and space borne radiometers. *Int. J. Remote Sens.*, Vol. **5**, 19-46.
- Rudman, S., R.W. Saunders, C.J. Kilsby and P.J. Minnett, 1994. Water vapour continuum absorption in mid-latitudes: aircraft measurements and model comparisons. *Q. J. R. Met. Soc.*, **120**, 795-807.
- Saunders, R.W. and P.J. Minnett, 1990. The measurement of sea surface temperature from the C-130. MRF Internal Note No. 52. Meteorological Research Flight, Royal Aerospace Establishment, Farnborough, Hampshire, U.K., 16pp.
- Schluessel, P., H-Y Shin, W.J. Emery and H. Grassl, 1987. Comparison of satellite-derived sea-surface temperature with in-situ skin measurements. *J. Geophys. Res.*, **92**, 2859-2874.
- Schluessel, P., W.J. Emery, H. Grassl and T. Mammen, 1990. On the bulk-skin temperature difference and its impact on satellite remote sensing of sea surface temperatures. *J. Geophys. Res.*, **95**, 13,341-13,356.
- Schmidlin, F.J., 1988. WMO International radiosonde intercomparison phase II, 1985. Instrument and Observing Methods, Report No 29. WMO/TD 312. World Meteorological Organization, Geneva. 113pp.
- Schwalb, A., 1973 Modified version of the improved TIROS operational satellite (ITOS D-G). NOAA TM NESS 35. Available from NTIS as COM-72-10547. 48 pp.
- Schwalb, A., 1978 The TIROSN/NOAA A-G satellite series. NOAA TM NESS **95**. Available from NTIS. 75 pp.

- Selby, J.E.A., F.X. Kneizys, J.H. Chetwynd Jr., and R.A. McClatchey, 1978. Atmospheric Transmittance/Radiance: Computer Code LOWTRAN 4. AFGL-TR-78-0053, *Environmental Research Papers*, No. 626. Available from NTIS.
- Shenk, W.E. and V.V. Salomonson, 1972. A multispectral technique to determine sea surface temperature using NIMBUS II data. *J. Phys. Oceanogr.* **2**, 157-167.
- Smith, A.H., R.W. Saunders and A.M. Zavody, 1994. The validation of ATSR using aircraft radiometer data over the Tropical Atlantic. *J. Atmos. and Oceanogr. Techn.* 789-800.
- Smith, W.L., R.O. Knuteson, H.E. Revercombe, W. Feltz, H.B. Howell, W.P. Menzel, N.R. Nalli, O. B. Brown, J. Brown, P.J. Minnett and W. McKeown, 1996. Observations of the infrared radiative properties of the ocean - implications for the measurement of sea-surface temperature via satellite remote sensing. *Bull. Am. Met. Soc.*, **77** (1), 1996, 41-51.
- Stokes, G.M. and S.E. Schwartz, 1994. The atmospheric Radiation Measurement (ARM) Program: Programmatic Background and Design of the Cloud and Radiation Test Bed. *Bull. Am. Met. Soc.*, **75**, 1201-1221.
- Stramma, L., P. Cornillon, R.A. Weller, J.F. Price and M.G. Briscoe, 1986. Large diurnal sea surface temperature variability: satellite and *in situ* measurements. *J. Phys. Oceanogr.*, **16**, 827-837.
- Strong, A.E. and E.P. McClain, 1984. Improved ocean surface temperature from space - comparisons with drifting buoys. *Bull. Am. Meteor. Soc.* **65**(2), 138-142.
- Susskind, J., J. Rosenfield, D. Reuter, and M.T. Chahine, 1984. Remote sensing of weather and climate parameters from HIRS2/MSU on TIROS-N. *J. Geophys. Res.*, **89**(C6), 4677-4697.
- Walton, C.C., 1988. Nonlinear multichannel algorithms for estimating sea-surface temperature with AVHRR satellite data. *J. Appl. Meteor.* **27**, 115-124.
- Walton, C.C., E.P. McClain and J.F. Sapper, 1990. Recent changes in satellite-based multi-channel sea surface temperature algorithms. Preprint, Marine Technology Society Meeting, MTS '90, Washington DC, September 1990.
- Weller, Robert A. and Peter K. Taylor, 1993. Surface Conditions and Air-Sea Fluxes, CCCO-JSC Ocean Observing System Development Panel, 131 pp. Texas A&M University, College Station, TX 77843-3146.
- WOCE, 1985. WOCE Global Air-Sea Interaction Fields, ed. W.G. Large, US WOCE Technical Report No. 1, September 1985, 36 pp.

Zavody, A.M., C.T. Mutlow, and D.T.Llewellyn-Jones, 1995. A radiative transfer model for sea surface temperature retrieval for the Along-Track Scanning Radiometer, *J. Geophys. Res.*, **100**, 937.